Laser pyrolysis fabrication of ferromagnetic γ'-Fe_4N and FeC nanoparticles

C. A. Grimes[a)]
Department of Electrical Engineering, The University of Kentucky, Lexington, Kentucky 40506

D. Qian and E. C. Dickey
Department of Chemical and Materials Engineering, The University of Kentucky, Lexington, Kentucky 40506

J. L. Allen
Center for Applied Energy Research, The University of Kentucky, Lexington, Kentucky 40506

P. C. Eklund
Department of Chemical and Materials Engineering and Department of Physics and Astronomy, The University of Kentucky, Lexington, Kentucky 40506

Using the laser pyrolysis method, single phase γ'-Fe_4N nanoparticles were prepared by a two step method involving preparation of nanoscale iron oxide and a subsequent gas–solid nitridation reaction. Single phase Fe_3C and Fe_7C_3 could be prepared by laser pyrolysis from $Fe(CO)_5$ and $3C_2H_4$ directly. Characterization techniques such as XRD, TEM and vibrating sample magnetometer were used to measure phase structure, particle size and magnetic properties of these nanoscale nitride and carbide particles. © *2000 American Institute of Physics.* [S0021-8979(00)38408-0]

I. INTRODUCTION

There is growing interest in nanoscale nitride and carbide particles for potential application as catalysts, sensors, EMI shielding materials, magnets, etc. Laser driven pyrolysis of organometallic precursors is a general synthetic tool allowing the synthesis of nanoscale particles ranging from 2 to 20 nm at rapid heating and cooling rates ($\approx$ 100 000 °C/s).[1,2] Figure 1 is a schematic drawing of the laser pyrolysis system; the reactive chemical components are carried by an inert gas into the laser heated reaction zone where the particles are formed. Particle size is controlled by changing the flow rate of the chemicals through the pyrolysis reaction zone. Laser pyrolysis of organometallic precursors in the presence of ethylene, ammonia, and oxygen has, in the past, allowed the successful synthesis of carbides (WC_x), oxycarbides ($Mo_2C_xO_y$), oxynitrides ($Mo_2N_xO_y$), sulfides (MoS_2,CoS_2), and oxides (TiO_2).[2]

Fine iron nitride particles have been prepared from different precursors such as: (1) α-Fe powders by high energy ball milling and additional low temperature annealing;[3,4] (2) Fe_2O_3 powders by gas–solid nitridation reaction in NH_3/H_2 atmosphere;[5,6] and (3) $Fe(CO)_5$ pyrolysis in a nitriding atmosphere (NH_3 or NH_3/H_2).[1,3,7,8] However methods (1) and (3) suffer from the inability to prepare pure single phase nanoscale nitride particles, and method (2) is a complicated process for which sample quality is difficult to maintain. Experimental attempts to prepare iron nitrides via pyrolysis of iron pentacarbonyl in a nitriding atmosphere (ammonia) also led to mixed phase materials within the available parameter space of pressure, flow rates, and gas composition. In this paper we report on a two step method for fabrication of single phase Fe_4N nanoparticles, involving preparation of nanoscale iron oxide and a subsequent gas–solid nitridation reaction.

II. EXPERIMENTAL METHOD

A. Synthesis of Fe_3C, Fe_7C_3, and Fe_4N nanoparticles

Iron carbide nanoparticles were synthesized via laser pyrolysis, using $Fe(CO)_5$ as the precursor, as previously described:[1] Ethylene, C_2H_4, was bubbled through a room temperature reservoir of the liquid precursor to produce a stream of $Fe(CO)_5$ laden gas which was directed into the laser pyrolysis reaction chamber in which a CO_2 laser perpendicularly intersects the gas, producing iron carbides via pyrolysis. Buffer Ar gas was added to the chamber to columnize the flow of particles from the chamber and to maintain a specific pressure which determines the finally obtained phase: at pressure$<$200 Torr α-Fe is obtained, while Fe_3C and Fe_7C_3 are obtained at 300 and 500 Torr, respectively. The proposed reactions can be written as:

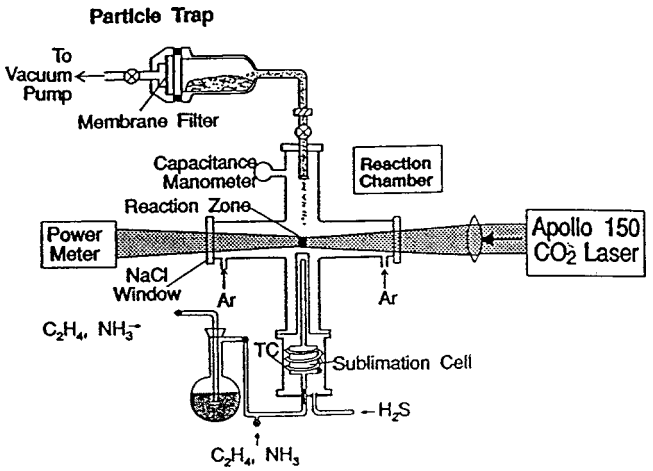

FIG. 1. Schematic drawing of laser pyrolysis system.

[a)]Author to whom correspondence should be addressed; electronic mail: grimes@engr.uky.edu

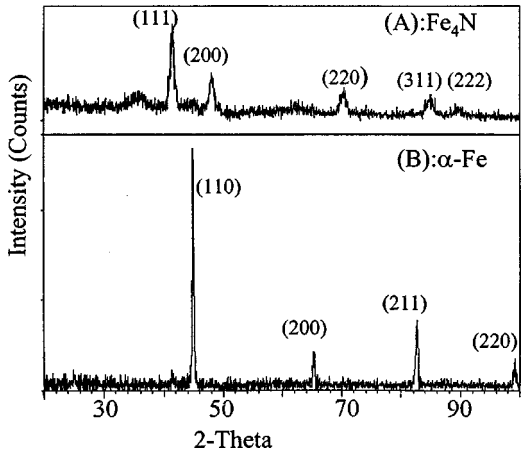

FIG. 2. X-ray diffraction patterns of Fe_4N powders. (A) γ'-Fe_4N (before annealing). (B) α-Fe (after annealing, γ'-Fe_4N has decomposed into α-Fe).

$$6\,Fe(CO)_5 + C_2H_4 \Rightarrow 2\,Fe_3C + 30\,CO + 2\,H_2$$

$$14\,Fe(CO)_5 + 3\,C_2H_4 \Rightarrow 2\,Fe_7C_3 + 70\,CO + 6\,H_2.$$

To prepare single phase Fe_4N nanoparticles the synthesis was performed in a two-step fashion: infrared laser-driven pyrolysis of iron pentacarbonyl $Fe(CO)_5$ in an oxidizing environment (800 ccm/s Ar, 57 ccm/s C_2H_4, and 118 ccm/s O_2) was used to obtain single phase hematite (Fe_2O_3)[9] nanoparticles. Ethylene absorbs the IR laser radiation and thus serves to promote the dissociation of iron pentacarbonyl and subsequent oxidation. The iron oxide nanoparticles were ramped from room temperature to 425 °C at 1°/min then held at 425 °C for 1 h, with a flowing atmosphere of NH_3/42%–47% H_2 to produce single phase Fe_4N. Synthesis of Fe_4N nanoparticles from the oxides involves a reduction of the oxide to the metal followed by subsequent nitridation with NH_3. The most probable reactions are:

$$Fe_2O_3 + 3H_2 \Rightarrow 2\,Fe(s) + 3\,H_2O$$

$$8\,Fe + 2\,NH_3 \Rightarrow 2\,Fe_4N + 3\,H_2.$$

The resulting powder was then then removed from the laser pyrolysis reaction chamber and placed in a quartz reactor under a flow of 45 vol %H_2 and 55 vol %NH_3, as measured by calibrated mass flow controllers. The temperature was ramped at 1°/min to 425 °C and held at this temperature for 12 h. The heating ramp rate was controlled in order to prevent a runaway reaction which would sinter the particles excessively. A higher dwell temperature was favored to form Fe_3N rather than Fe_4N.

B. Characterization techniques

X-ray diffraction (XRD) was used to determine the phase structure and calculate the particle size according to Scherrer relationship $d = 0.9\lambda/(B\cos\theta)$, where d is the diameter of nanoparticle in angstroms, B is the half maximum line width, and λ is the x-ray wavelength. Particle size and morphology were investigated by TEM. The TEM samples were prepared by first dispersing the particles in alcohol using ultrasonic excitation, then transferring the nanoparticles onto the copper grid with carbon support film. A vibrating sample magnetometer (VSM) was used to measure the magnetic properties of the nanoparticles over the temperature range −200–800 °C.

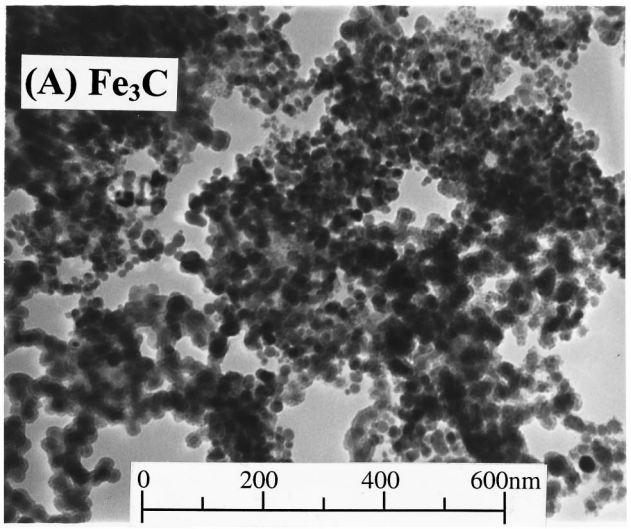

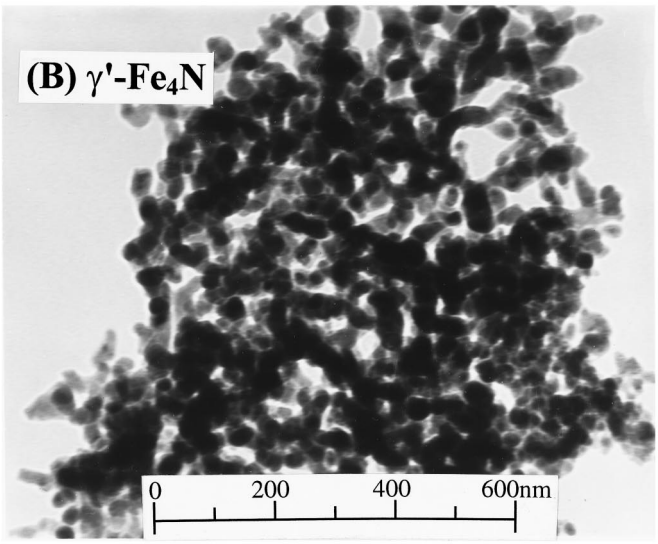

FIG. 3. TEM image of nanoparticles (A) Fe_3C, (B) γ'-Fe_4N.

III. RESULTS AND DISCUSSION

A. Phase structure and particle size

XRD results indicate our ability to fabricate single phase Fe_3C,Fe_7C_3 and γ'-Fe_4N particles. Earlier work reported on the XRD characterization of the Fe_3C and Fe_7C_3 nanoparticles. A typical XRD pattern of γ'-Fe_4N particles is shown in Fig. 2(a). According to the Scherrer relationship, $d = 0.9\lambda/B\cos\theta$, for the (111) peak $2\theta = 41.166$, and an average γ'-Fe_4N particle size of 19.15 nm is calculated.

Figure 3 shows TEM images of Fe_3C and γ'-Fe_4N particles, with average particle sizes of 20 and 35 nm, respectively; values larger than those predicted from XRD calculations. As the Fe_3C and γ'-Fe_4N nanoparticles are ferromagnetic, one possible explanation of the difference between calculated and observed particle sizes is due to particle aggregation under the influence of the electromagnetic field

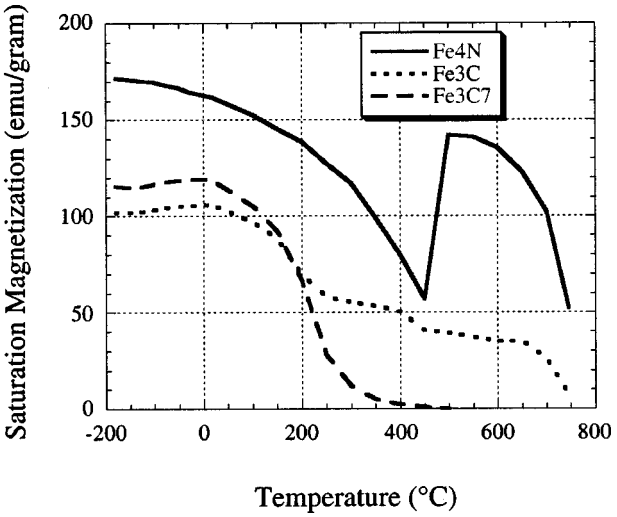

FIG. 4. Saturation magnetization of Fe_3C, Fe_7C_3, and γ'-Fe_4N nanoparticles as a function of temperature.

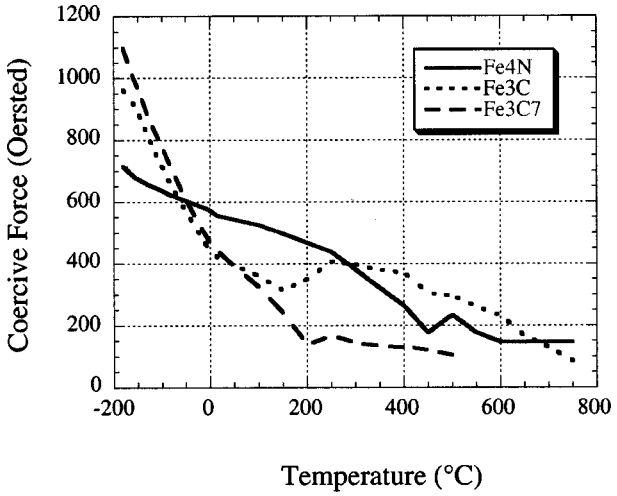

FIG. 5. Coercive force of Fe_3C, Fe_7C_3, and γ'-Fe_4N nanoparticles as a function of temperature.

in the TEM. Referring to Fig. 3, it is worth noting that the Fe_3C particles have a spherical shape while the γ'-Fe_4N particles look rectangular.

B. Magnetic properties

Figures 4 and 5 show, respectively, the saturation magnetization ($4\pi Ms$) and coercive force of Fe_3C, Fe_7C_3, and γ'-Fe_4N nanoparticles as a function of temperature. The saturation magnetization value of the γ'-Fe_4N nanoparticles is obviously higher than either Fe_3C and Fe_7C_3. Sakuma[10] concluded that the major role of the interstitial nitrogen atoms is to expand the Fe (fcc) lattice to enhance the magnetic moments. At 298 °K, γ'-Fe_4N nanoparticles exhibit saturation magnetization of 165 emu/g, which is close to the value of bulk Fe_4N material (184 emu/g).[7]

There is a sharp change in Fig. 4 at about 450 °C which corresponds to the γ'-Fe_4N particles decomposing into α-Fe and nitrogen; this is confirmed by XRD, as shown in Fig. 2(b). As discussed in Ref. 6, γ'-Fe_4N decomposes into α-Fe and nitrogen before reaching the Curie temperature T_c which is predicted theoretically at 490 °K. This decomposition makes it difficult to determine the Curie temperature from the $4\pi Ms-T$ curve because of the larger magnetic moment contribution from α-Fe.

Maximum coercive force values are obtained when the particle size drops below the single domain limit. However, as the particle size continues to decrease below the single domain value, the spins are increasingly affected by thermal fluctuations and the particles will finally become superparamagnetic. Particles with significant shape anisotropy can remain single domain to much larger dimensions than their spherical counterparts.[11] The γ'-Fe_4N nanoparticles, Fig. 3(b), are seen to be bar-like in shape, having larger shape anisotropies than spherical particles, which may help to explain why the 35 nm γ'-Fe_4N particles exhibit a coercive force comparable to that of 20 nm Fe_3C particles. Mossbauer and magnetization measurements show that 15 nm γ'-Fe_4N nanoparticles are superparamagnetic ($4\pi Ms \approx 5$ emu/g), while 22 nm γ'-Fe_4N nanoparticles are ferromagnetic ($4\pi Ms \approx 180$ emu/g).[6] Hopefully our work will provide other researchers with a synthesis framework in which to obtain single phase γ'-Fe_4N nanoparticles sized to exactly support a single domain.

IV. CONCLUSIONS

Using a laser pyrolysis method single phase γ'-Fe_4N nanoparticles were prepared by a two step method involving preparation of nanoscale iron oxide and a subsequent gas–solid nitridation reaction. Single phase Fe_3C and Fe_7C_3 could be prepared by laser pyrolysis from $Fe(CO)_5/3C_2H_4$ directly. Characterization techniques such as XRD, TEM, and VSM were used to measure phase structure, particle size, and magnetic properties of these nanoscale nitride and carbide particles.

ACKNOWLEDGMENTS

This work was supported under NSF Contract No. EPS-9452895 and NASA Contract No. NAG5-4594.

[1] C. A. Grimes, J. L. Horn, G. G. Bush, J. L. Allen, and P. C. Eklund, IEEE Trans. Magn. **33**, 3736 (1997).
[2] R. Ochoa, X. Bi, A. M. Rao, and P. C. Eklund, in *The Chemistry of Transition Metal Carbides and Nitrides*, edited by S. T. Oyama (Chapman and Hall, London, England, 1996), pp. 489–510.
[3] W. A. Kaczmarek, Scr. Metall. Mater. **33**, 1687 (1995).
[4] P. Y. Lee, T. R. Chen, and T. S. Chin, J. Alloys Compd. **222**, 179 (1995).
[5] X. Bao, R. M. Metzger, and W. D. Doyle, J. Appl. Phys. **73**, 6734 (1993).
[6] R. N. Panda and N. S. Gajbhiye, IEEE Trans. Magn. **34**, 542 (1998).
[7] X. Q. Zhao, Y. Liang, F. Zheng, Z. Q. Hu, G. B. Zhang, and K. C. Bai, Mater. Res. Soc. Symp. Proc. **368**, 39 (1995).
[8] X. Bi, B. Ganguly, G. P. Huffman, F. E. Huggins, M. Endo, and P. C. Eklund, J. Mater. Res. **8**, 1666 (1993).
[9] B. J. Jonsson, T. Turkki, V. Strom, M. S. El-Shall, and K. V. Rao, J. Appl. Phys. **79**, 5063 (1996).
[10] A. Sakuma, J. Appl. Phys. **79**, 5570 (1996).
[11] D. L. L. Pelecky and R. D. Rieke, J. Chem. Mater. **8**, 1770 (1996).